Pergamon

0273-1177(95)00467-X

Adv. Space Res. Vol. 16, No. 11, pp. (11)47–(11)50, 1995

0273–1177/95 $9.50 + 0.00

ALGORITHMS FOR GROUND BASED OPTICAL DETECTION OF SPACE DEBRIS

T. Schildknecht, U. Hugentobler and A. Verdun

Astronomical Institute, University of Bern, Sidlerstrasse 5, CH-3012 Bern, Switzerland

ABSTRACT

Optical detection of space debris is a technical challenge from the point of view of the observations as well as of the data processing. The most promising technique for ground based optical observations consists of using CCD detectors in combination with specially tuned digital image processing techniques.

We present observation scenarios and image processing algorithms allowing to recognize the faint trailed images of the moving debris in front of the stellar background. After a discussion of the detection limits the technique will be illustrated by observations of a debris object in the geostationary ring.

INTRODUCTION

From the observational point of view, the most important characteristics of artificial satellites and space debris are the objects' apparent magnitude and angular velocity. Values for typical representatives of satellites in four different orbit categories are listed in Table 1. The table includes

TABLE 1 Fast Moving Objects: Observational Characteristics

			ECS4	GPS	LAGEOS	ERS1
Altitude		[km]	36 000	20 000	6000	750
Size		[m x m]	2x14	3x5	0.6x0.6	3x12
Max. Motion		[arcs s^{-1}]	15	30	240	2000
Magnitude		[m_v]	11	8 – 14	14	< 6
Pixel Crossing Time	SLR	[ms]	273	138	17	2
	ZIMLAT		66	33	4	0.5
FOV Crossing Time	SLR	[s]	140	70	9	1
	ZIMLAT		200	100	13	1.5
Illuminance	SLR	[ph s^{-1}]	70 800	> 4470	4470	$> 7 \cdot 10^6$
	ZIMLAT		346 000	> 21 800	21 800	$> 3 \cdot 10^7$

values for the existing 0.5 m SLR telescope at the Zimmerwald observatory and for the planned 1 m combined Zimmerwald Laser Ranging and Astrometric Telescope (ZIMLAT) which should become operational in late 1995. We currently use a 512 x 512 pixel CCD camera in the $f/2$ prime focus of the SLR telescope which results in a pixel size of 4.″1 and a field of view of about 35′. The pixel size of the $f/4$ focus of the ZIMLAT telescope will be about 1″ and the field of view about 50′.

The European Space Agency (ESA) is installing a 1 m Zeiss telescope of the Ritchey-Crétien type on the Canary Islands. It should be operational at beginning of 1996. One of the tasks the instrument is designed for is the search for space debris using the $f/4$ Ritchey-Crétien focus with a field of view of 1.2°. The focal plane assembly will contain a 4096 x 4096 pixel CCD mosaic. A full frame from this sensor consists of 32 MB of data! The corresponding readout time will be of the order of 40 s (depending on the number of parallel output channels). The processing of such data rates (the exposure times are of the order of one second and thus negligible) is a technical challenge: the algorithms must be rapid, i.e. simple and efficient.

OBSERVATION STRATEGIES AND DETECTION TECHNIQUES

Several techniques are feasible to detect objects moving with respect to the stars. One such technique consists of a search for objects with different characteristics than stars, e.g. for elongated images on a siderostatically tracked frame. A different, less time consuming, method is the comparison of the current frame with a reference frame. We will discuss two approaches (which may be combined), the 'masking technique' and the 'frame subtraction technique'.

In the first technique a reference frame is used to generate a mask covering every object found on the frame. For each object the digital mask is made slightly larger than the original object image itself. The subsequent search frames are then scanned using this mask. Consequently only the portion of the frame that contains no stars must be searched for unknown objects. One and the same reference mask may be applied for a long time interval if siderostatic tracking is used. In the earth-fixed horizon system this corresponds to a scanning of a strip in the sky (e.g. for the search of geostationary objects). The time necessary to generate the mask is negligible in this case. If the search is performed with a fixed telescope, the mask has to be extended continuously to the east. In Figure 1 an example of a reference frame, the corresponding mask and a masked search frame containing a satellite is shown.

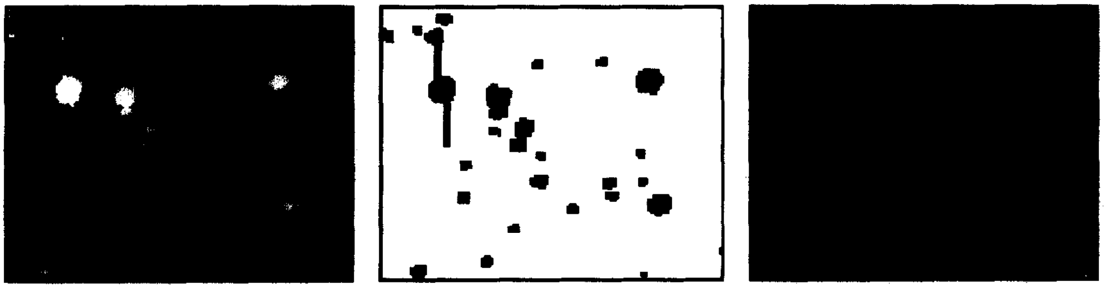

Fig. 1. Reference image (left), reference mask (middle), and masked image (right) with the Meteosat 4 apogee boost motor showing up. The images were taken with the Zimmerwald SLR telescope. The field is 14' x 10' and the exposure time was 1.5 s.

In the second approach the difference of consecutive frames or the difference of the current frame and a reference frame is used to search for objects. In this case is not necessary to model the sky background — an advantage of this method. The two frames must however be transformed in such a way that the stars on the two frames coincide. Processing time may allow only for translations by an integer number of pixels. To keep the noise at a low level, the average of several frames might be used to generate the reference frame. Bright stars which usually do not completely disappear in the difference of two frames may be masked thus using a combination of the masking and the image subtraction technique.

During the object search process (on the masked or the differenced frames) the following questions have to be answered: a) is there a moving object on the frames and (if yes) where is it and b) which pixels belong to the object. Both questions may be treated with thresholding algorithms which require, however, a good model for the sky background. By using filter algorithms the threshold may be as low as the standard deviation of the background above the mean background taking advantage of intensity correlations of neighbouring pixels belonging to an object /1/.

The signal-to-noise ratio of faint objects may be increased by tracking with the expected motion of the objects of interest. In order to increase the detection probability, the search should be performed at the point of slowest motion, e.g. at the culmination point for geostationary objects with non-zero orbital inclination or at the apogee for GTO objects.

If the orbital plane is known — e.g. when looking for debris of an exploded upper stage or satellite a few days after disintegration — the search can be carried out along-track while tracking with the expected motion.

SIGNAL-TO-NOISE RATIO AND DETECTION LIMIT

To derive detection limits as a function of object brightness, exposure time and sky brightness for point sources or moving objects, the signal-to-noise ratio S/N on the detector has to be studied. The signal-to-noise ratio for a CCD detector may be written as

$$\mathrm{S/N} = \frac{\dot{S}_o t}{\sqrt{\dot{S}_o t + m\left((\dot{S}_s + \dot{S}_d)t + S_r\right)}}, \tag{1}$$

where $\dot{S}_o$ represents the mean signal associated with the object (in photons per second) as registered by the detector, $\dot{S}_s$ and $\dot{S}_d$ are the signal due to the mean sky background and the mean detector dark current (in photons per second and pixel) respectively, S_r is the square of the detector system readout noise (in equivalent photons per pixel, i.e. the variance of the Poisson distribution), t is the exposure time in seconds, and m the number of pixels over which the source is extended. The area m over which the object is detected is not a well defined quantity. It depends on the algorithm used to detect the object pixels (e.g. the threshold setting) and the noise level itself. The minimal signal-to-noise ratio of a detectable object is of the order of 2-5 for thresholding algorithms.

For a point source of given intensity, the signal-to-noise ratio always grows with increasing exposure time. If the readout noise is negligible, the exposure time grows with the square root of the (requested) signal-to-noise value. In the object dominated regime the signal-to-noise ratio is inversely proportional to the object intensity, in the regime dominated by the sky background it is inversely proportional to the square of the intensity and proportional to the sky brightness.

The situation is different if the source is moving across the pixels during the exposure. The number of pixels m within the object's image is growing with time. Because the sky background is accumulating proportional to time too, the square root in equation (1) will, for long exposure times, be dominated by a background noise term proportional to t. The signal-to-noise ratio will then no longer increase with time. The intuitive reason for this behaviour is that before and after the passage of the object the pixels inside the object's trail collect only background noise. The maximum achievable S/N ratio is (see /3/)

$$s_\infty = \lim_{t\to\infty} s = \frac{\dot{S}_o}{\sqrt{\sqrt{m_o}\,v S_s}} \quad = \quad \frac{\dot{S}_o}{\sqrt{m_o \dot{S}_s}}\sqrt{t_o}, \tag{2}$$

where m_o is the number of pixels illuminated by the source at a given instant, v is the velocity of the source in pixels per second and $t_o = \sqrt{m_o}/v$ is the time the object's image needs to travel a distance equal to its width ('object crossing time').

We have to find out how soon this maximal S/N ratio is reached in order to define the minimum integration time. The time t_κ needed to achieve a certain fraction κ of the limiting signal-to-noise ratio is given by the relations

$$t_\kappa^o \approx \frac{\dot{S}_o}{m_o \dot{S}_s} \cdot \frac{t_o}{(\frac{1}{\kappa^2} - 1)}, \qquad t_\kappa^s \approx \frac{t_o}{\frac{1}{\kappa^2} - 1}, \qquad t_\kappa^r \approx \frac{S_r}{\dot{S}_s t_o} \cdot \frac{t_o}{(\frac{1}{\kappa^2} - 1)} \tag{3}$$

for the object dominated, the sky dominated and the readout noise dominated case respectively (for more information see /3/). To reach 90% of the maximum signal-to-noise ratio, a time $t_\kappa = 4.26 t_o$

is necessary, i.e., the object's trail must be about 4 times longer than its diameter normal to the along-track direction. Therefore an upper limit for the exposure time of the order of a few object crossing times is adequate.

RESULTS

We illustrate the technique using observations of the Meteosat 4 apogee boost motor (COSPAR designation 89020E) made at the Zimmerwald observatory. The boost motor body with a size of 1.3 m x 0.8 m was observed on April 30, May 3 and June 30, 1994. One of the frames from June 30 is reproduced in Figure 1. The image of the object (the frame was exposed for 1 s) contains about 1000 photons. The signal-to-noise ratio in the 9 pixels detected is 12. From the data of several nights a mean object brightness of the order of 15 m_v to 16 m_v was estimated. From the brightness and the mean cross section of 1 m^2 we derive an albedo of about 0.2 (a reasonable value for an object of this type).

From the two first nights, each containing two observations, an orbit was determined. The eccentricity and the argument of perigee were kept fixed at the value given in the ESA log of geostationary objects /5/. The remaining elements together with formal errors and elements from the ESA log are given in Table 2. The rms of the observations was $0''.7$. Using the elements based on this three days interval, the orbit was extrapolated for two months with numerical integration and the object was found at a distance of 2' from the computed position.

TABLE 2 Computed Osculating Elements of Meteosat 4 Apogee Boost Motor

Epoch of elements: 1994-Apr-30, 0:00UT	elements		formal errors	ESA log /5/
Semimajor axis	42124212.02m	±	5.60m	42123950.28m
Inclination	3.381527°	±	.000696°	3.376771°
R.A. of ascending node	56.451822°	±	.002513°	55.780751°
Longitude at osculation epoch	214.3736780°	±	.000187°	214.3773237°

SUMMARY AND CONCLUSIONS

Time-optimized, automated search algorithms for the detection of space debris in GEO and GTO orbits haven been developed. The optimum search scenario consists of a) short exposures (0.5 to 5 seconds) while tracking with the expected velocity of the objects and b) repositioning of the telescope between the exposures to catch up with the sidereal motion. Using the 0.5 m SLR telescope at Zimmerwald known GEO objects with sizes down to 1 m^2 are routinely detected. The smallest unknown (near) GEO object found with this instrument has a size of the order of 0.25 m^2 (inferred from its apparent magnitude). For the new 1 m ZIMLAT telescope (operational in fall 1995) in combination with the optimized detection algorithms we expect a detection limit which is about 15 times lower (i.e. at about 0.017 m^2 corresponding to an object diameter of about 0.15 m).

REFERENCES

1. T. Schildknecht, U. Hugentobler, A. Verdun, G. Beutler, Ground Based Optical Observations of Space Debris Using CCD Techniques, in: *Proceedings of the First European Conference on Space Debris*, ed. W. Flury, ESOC, Darmstadt 1993, p.85. 2. A. Verdun, Objekterkennung und Zentroidbestimmung bei CCD-Richtungsbeobachtungen, Lizentiatsarbeit, Universität Bern, 1993. 3. T. Schildknecht, Optical Astrometry of Fast Moving Objects Using CCD Detectors, Ph.D. thesis, University of Bern, 1994. 4. T. Schildknecht, U. Hugentobler, CCD Astrometry of Artificial Satellites, in: *Conference on Dynamics and Astrometry of Natural and Artificial Celestial Bodies*, ed. I. Wytrzyszczak, Poznań, in press (1994). 5. G. Janin: Log of Objects Near the Geostationary Ring, ESOC, Darmstadt, April 1994.